Advanced Ceramics Progress: Vol. 6, No. 4, (Autumn 2020) 28-36

Advanced Ceramics Progress

Research Article

Journal Homepage: www.acerp.ir

Lithium Substitution Glass Composition Used in Glass Ionomer Cement: Physiochemical Properties in Artificial Saliva

T. Mohammadi Hafshejani [a], A. Zamanian [a], A. Faeghinia [b] *

[a] *Department of Nanotechnology and Advance Materials, Materials and Energy Research Center, Meshkindasht, Alborz, Iran*
[b] *Department of Ceramic, Materials and Energy Research Center, Meshkindasht, Alborz, Iran*

ARTICLE INFO

Article History:

Received 11 August 2020
Received in revised form 7 September 2020
Accepted 4 October 2020

Keywords:

Glass Ionomer
Cement
Lithium
Antibacterial Property
Sodium

ABSTRACT

In this study, glasses with 41.6 SiO_2, 28.5 Al_2O_3, 15.5 CaF_2, 3.7 $AlPO_4$, 1.5 AlF3, (9.2-X) NaF, and X LiF (X= 0, 3, 6, and 9.2) compositions were prepared. Fourier Transform Infrared Spectroscopy (FTIR) showed the red shift of Si-O-Si vibration mode by Lithium substitutions. According to the results of Differential Thermal Analysis (DTA), ΔT_g = 60 ºC was proved by the lithium substitution. Field Emission Scanning Electron Microscopy (FESEM), antibacterial property, glass solubility in Artificial Saliva (AS), and pH variation in AS by dissolution were measured. Following the initial substitution of lithium, the glass density was reduced from 2.62 to 2.40 g/cm^3, whereas in the 6 wt. % Li concentration, the high field strength played the main role and the density increased from 2.40 to 2.58 g/cm^3. In artificial saliva with basic pH, the durability of Li bearing glasses increased and the degradation rate decreased. Durability decreased in the acidic environment. By increasing the Li substitution, the antimicrobial property of the cement was enhanced.

https://doi.org/10.30501/acp.2020.243433.1041

1. INTRODUCTION

Glass Ionomer Cements (GICs) have drawn considerable interest by those specializing in the field of dentistry over the last 50 years [1]. GICs are used in restorative dentistry as the filling materials, luting, and lining cements [2, 3]. A contributing factor is fluoride ion release. Fluoride prevents cavity progression and helps maintain adequate physical properties for chewing [3].

Additional factors include the low thermal expansion coefficient similar to the tooth structure which gives rise to the thermal compatibility of this glass with the tooth enamel. The setting reaction has low exothermic energy and GICs chemically bond with enamel and dentin. Close module coefficient with dentin, biocompatibility, and low cytotoxicity all play significant roles [4]. They are usually used in pediatric dentistry as filling, especially when micro-invasive approaches are selected instead of conventional methods for fixing the dental caries [5].

GICs are formed by mixing glass powder made of acid degradable fluoro-aluminosilicate and an ionomer with carboxylic acids, usually polyacrylic acid and copolymers of polyacrylicacid. In addition, they are formed with the reaction of liquid polyacid ionomer and the calcium released glass (forming insoluble polysalts) [5].

The decomposition of glass network by acid attack causes the release of aluminum and calcium from the outer layer of filler particles and it determines the crosslinking degree of the poly salt matrix [6-8]. Alkali metals are the main components of the powder, reduce the melting temperature, and form Non-Bridging Oxygens (NBOs) in the cement matrix as network modifiers [9, 10]. Incorporation of sodium in the glasses has diverse effect on some mechanical and physical properties [11]. When glass is under acid attack since Na^+ is more susceptible (less resistant or weaker) against acid

* Corresponding Author Email: a.faeghinia@merc.ac.ir (A. Faeghinia)

URL: http://www.acerp.ir/article_122884.html

Please cite this article as: Mohammadi Hafshejani, T., Zamanian, A., Faeghinia, A., "Lithium Substitution Glass Composition Used in Glass Ionomer Cement: Physiochemical Properties in Artificial Saliva", ***Advanced Ceramics Progress***, Vol. 6, No. 4, (2020), 28-36

attack, Na^+ competes with Ca^{2+} and Al^{3+} in carboxylate groups [12].

Therefore, in view of all the factors considered, it can be concluded that the numbers and concentration of sodium ions should be low for cements.

It has been asserted that internal cracks and air bubbles in these cements cause micro-leakage [13-15]. Several strains of oral streptococci and bacteria, which can penetrate by micro-leakage, may lead to the dental plaque biofilms formation and thus, play a major role in the development of caries [16-19].

Lithium is an antibacterial metal and its antiviral and anti-parasitic properties have been previously shown [20-26]. It has been demonstrated that bioactivity in bio glass was increased by significant lithium addition [27]. Wang et al. developed the bio glass (55% Si_2O- 36% CaO- 4% P_2O_5- 5 Li_2O) with 5 wt.% Lithium with positive effect on mesenchyme cell proliferation and improved the antibacterial properties [28]. Further, it was stated that by using lithium carbonate, the bone mass would be increased [29]. In addition, the small molar weight of this ion reduced the density and solubility of glass in water [30-31].

However, the LiF effect on glass density, characteristic temperatures, glass structure, and finally acidic and basic resistance of GIC powder have not been studied before. In this work, the effect of substitution of NaF with different LiF concentrations on antibacterial properties and degradation of formed cements in acidic and basic environments is evaluated, which to the best of the authors' knowledge, the pH of environment has not been studied from the viewpoint of antibacterial properties before.

2. MATERIALS AND METHODS

2.1. Glass Synthesis

Four series of glass compositions based on 41.6 SiO_2, 28.5 Al_2O_3, 1.5 AlF_3, 3.7 $AlPO_4$, 15.5 CaF_2, (9.2-X) NaF, and X LiF were prepared with X= (0, 3, 6, and 9.2) and the samples were denoted by G1, G2, G3, and G4, respectively. The details of chemical composition of glasses are given in Table 1.

TABLE 1. Glass Composition

Sample Code	Content of components, Wt.%						
	SiO_2	Al_2O_3	$AlPO_4$	AlF_3	CaF_2	NaF	LiF
G_1	41.6	28.5	3.7	1.5	15.5	9.2	-
G_2	41.6	28.5	3.7	1.5	15.5	6.2	3
G_3	41.6	28.5	3.7	1.5	15.5	3.2	6
G_4	41.6	28.5	3.7	1.5	15.5	-	9.2

The batches were melted in alumina crucibles at 1350-1550 °C for 2 h (heating rate: 10 °C/min). The dried frits were ground and sieved so that the appropriate particle size <35 µm could be determined.

2.2. Glass Characterization

2.2.1. X-ray Diffraction

The crystalline/amorphous state of the samples was analyzed by X-Ray powder Diffraction (XRD). The X-ray patterns were obtained using a Scintag X-ray diffraction spectrometer (XRD, Philips- PW3710, The Netherlands) with Cu (Kα), operating nickel filtered Cu Kα radiation in the range of $2\theta = 10° - 80°$.

2.2.2. Fourier Transform Infrared Spectroscopy

The Fourier Transform Infrared (FTIR) spectra (Spectrum RXI, USA) of the glasses were recorded in the range of 400 – 4000 cm^{-1} with a spectral resolution of 2 cm^{-1}. The pellets with 13 mm diameter were prepared by mixing 10 mg of each sample with 1000 mg of KBr. The spectrum of each sample represents an average of 20 scans, which were normalized to the spectrum of blank KBr pellet.

2.2.3. Differential Thermal Analysis (DTA)

The thermal behavior of glasses was measured by differential thermal analysis (STA 409 PC Luxxto, Netzsch-Gerätebau GmbH Germany). The samples were tested in a condition in which the air is flowing with an alumina crucible and heated up to 1000 ℃ with a heating rate of 10 ℃ /min.

2.2.4. Density Measurement

The true density of the glasses was measured by means of a pycnometer (Accupyc 1330 pycnometer, Micrometrics Instruments, Norcross, Georgia, USA) using helium gas that produced the structural (true) density.

2.2.5. Glass Solubility

In this method, 150 mg of each glass was weighed and then, immersed in 100 mL of Artificial Saliva (AS) with 3.5, 6.8, and 9.2 pH. The composition of AS solution was made according to the instructions from [31]: 100 mL of KH_2PO_4 (2.5 mM); 100 mL of Na_2HPO_4 (2.4 mM); 100 mL $KHCO_3$ (1.50 mM); 100 mL of NaCl (1.0 Mm); 100 mL of $MgCl_2$ (0.15 mM); 100 mL of $CaCl_2$ (1.5 mM); and 6 mL of citric acid (0.002 mM). All specimens were incubated at 37 °C. Following different immersion time interval, the samples were removed and the weight of each remaining powder was recorded as m_2. The mass change during storage in artificial saliva was calculated by:

$$M_g = (m_1 - m_{2(t)})/m_1 \times 100 \quad (1)$$

During reactivity tests in different AS, pH changes were also assessed by a pH-meter (Aldrich-Z654280, Mettler Toledo, GmbH, Seven Easy pH meter).

2.2.6. Particles Morphology Analysis

Particle morphology of glass containing 9.2% Li was measured by Field Emission Scanning Electron Microscopy (FESEM Zeiss-DSM950,Oberkochen, Germany) operating at 25 kV before and after soaking in artificial saliva at pH=9.5 for 14 days.

2.3. Antibacterial Activity

For antibacterial testing by Colony Form Units (CFU) method, samples were incubated with the suspension of S.mutans at (1.5×108) CFU. The antibacterial activity was conducted by the plate-counting method. A phosphate buffer solution (pH ~ 7.4) containing the bacteria was used. The sample-containing solutions were incubated at 37 °C under vibration agitation for up to 24 h. Some of the solutions were then cultured on Brain Heart Infusion (BHI) and incubated at 37 °C for additional 24 hr, and the exact number of discrete colonies was counted as the number of the remaining bacteria. Antibacterial activity (E) was calculated through the following equation:

$$E(\%)=[(A-B)/A]\times 100\% \quad (2)$$

where A= number of viable bacteria with control glass (G1) in the tray and B=number of viable bacteria with lithium bearing glasses in the tray.

2.4. Cellular Behavior

MTT (3-dimethylthiazol-2, 5-diphenyltetrazolium bromide) colorimetric assay was used for determining cytotoxicity of samples. Briefly, disc-shaped cement samples with 1.00 mm thickness and 10 mm diameter were prepared. The samples were washed by ultrasonification with sterile distilled water and kept in sterilized appropriate flasks after disinfecting under ultraviolet light. Cytotoxicity tests were performed with the human osteoblast (G-292) cells. Cells were seeds at density of 1.5×10^4 cell/mL in a 96-well plate containing RPMI culture medium with 10% FBS and 1% Pen Sterp antibiotic. Then, the culture medium was discarded and the media supplemented with cements extracts were added to each cell and diluted by factors of 2, 4, and 8 with standard culture medium. After 24 h of incubation of the cells with the extracts, the media were exchanged with 100 µL of conditioned culture media containing 10% MTT solution and kept for 4 h. Then, cultural media were removed and 100 µL of dimethyl sulfoxide (DMSO) was added for dissolving the resulting formazon. The absorbance was read at 570 nm using a micro plate reader (BIO-TEK Elx 808, Highland park, USA). The obtained values were expressed as a percentage of the control cells to which no discs were added. All tests were repeated three times.

2.5. Statistical Analysis

All experiments for determining antibacterial activity were performed in three replicates. Statistical analysis of the antibacterial activity was used by one-way ANOVA and Tukey tests. Also, the variation in pH and mass change data were analyzed by ANOVA. The $P<0.05$ level was considered statistically significant.

3. RESULTS AND DISCUSSION

The XRD patterns of amorphous phases with the control sample with similar patterns are presented in Figure 1.

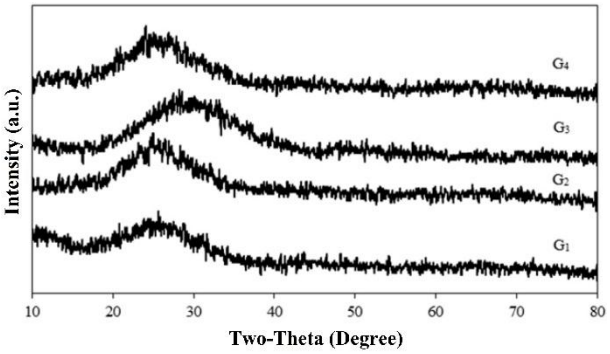

Figure 1. X-ray diffraction pattern of glass samples

The FTIR spectra of samples are illustrated in Figure 2. The high-frequency region, 800-1200 cm^{-1}, belongs to the asymmetric stretching mode of Si-O-Si. The frequency increases with the alkali compositions, suggesting greater stabilization with more efficient packing around Si-O-Si units, arising from an optimal mixing of Li^+ and Na^+ ions (G2 and G3). This could be confirmed by T_g results as well.

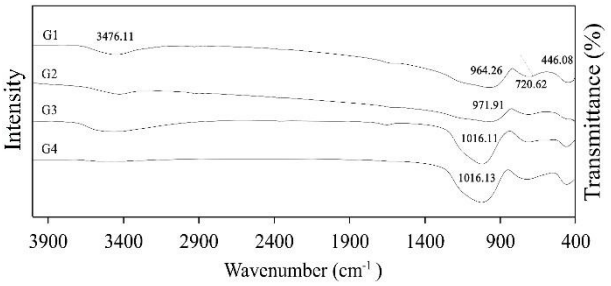

Figure 2. FTIR spectra of the investigated glasses

The peaks located at roughly 720 cm^{-1} are assigned to the Si-O-Si bridging oxygen atoms between the tetrahedra stretching [32], which have not changed clearly. Bands at 400-500 cm^{-1} could be attributed to the vibration of Si-O-Si and Al-O-Al [32]. Moreover, the weak bands at wave number 450 cm^{-1}might be associated with the vibration of the Li^+ cations [20].

Figure 3 shows the DTA results of glasses (G1, G2, G3, and G4). By the substitution of LiF to NaF composition, the T_g peaks shift to the higher temperatures.

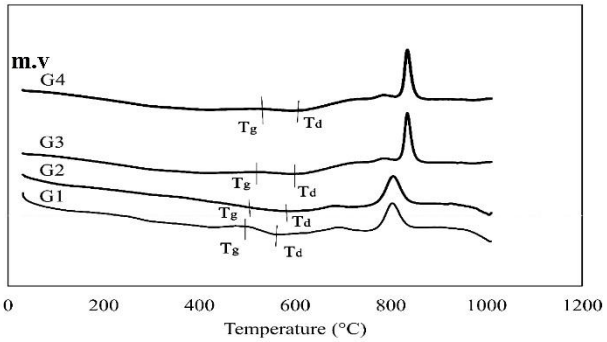

Figure 3. DTA curves samples (a):G1, (b):G2, (c):G3, and (d):G4

The transition temperatures, T_g (G4: 594ºC, G3: 588ºC, G2: 570ºC, and G1: 530ºC) and softening tempertures, T_d (G4: 627ºC, G3: 608ºC, G2: 592ºC, and G1: 570ºC) of the glasses shift to the higher temperatures by the substitution of Li. Moreover, the crystallization temperatures shift to the higher temperatures, too. The main reasons could be releated to the breaking of the silicate glasses network in the presence of Na, which is easier than Li [33].

Since Li^+ ions have smaller radii than Na^+ and higher field strength of 1.65 than Na^+ ions, the glasses become more compact upon the substitution of NaF with LiF (Althought the viscosity of glasses was supposed to be decreased).

Table 2 shows that G3 has higher density than G2 and G4.

As is well known, two main factors influence the density of a glass: the molecule weight of glass components and the other is the compactness of glass network. The decreases in density of glasses with the intial substitutions can be ascribed to the lower molecule weight of LiF. The increased density can be discribed by the high field strength of Li^+, resulting in a stronger link between glass structure and the compacted structure.

Due to the field strength of lithium ion, the lithium-oxygen bond in G3 is stronger than sodium-oxygen bond in G1. However, with further Li substitution (G4), the low atomic weight of Li causes decreased density. Thus, the results depend on the concentration of lithium. The atomic weight or strength field of this ion is the dominant factor.

It can be mentioned that the positive and negative effects of the substitutes on the glass structure are competing and non-monotonic changes in the glass properties with the substitutions are observed.

TABLE 2. Different densites obtained from glasses

Sample Code	Density (g/cm^3)
G_1	2.62±0.02
G_2	2.47±0.05
G_3	2.58±0.05
G_4	2.40±0.01

Colony count method was used for the determination of antimicrobial activity. The antibacterial effect was reported quantitatively after close contact of cements with the S.mutans suspension. To ensure the reliability of this experiment, three samples were used for each cement. Based on the results, G4 showed a comparably greater antibacterial effect than G1 and it correlated with the lithium amount as compared to the other samples. Thus, the greatest degree of the cement's antibacterial activity is directly related to the lithium amount. The greatest inhibition of S.mutans growth depends on the high level release of the antibacterial agent from the cements; therefore, with further time interval, the antibacterial activity increased, too. Also, lithium was released steadily and, therefore, the antibacterial activity was durable and time dependent.

According to Figure 4, the antibacterial activities were effectively enhanced by the concentrations of the added disinfectant ($p<0.05$). G4 exhibits the highest value (99.17 %.) of antibacterial activity.

Figure 4 and Table 3 show that the greatest inhibition of S.mutans growth depends on the high level release of antibacterial agents from the glass.

Figure 5 shows that the mechanism of glass dissolution depends on the pH of environment. At an acidic pH, an ion exchanging between network modifiers in the bulk of the glass and the protons in the solution is the main reaction.

Figure 6 shows the pH of immersed glasses in the AS at immersion time. The differences between the soaked samples in AS at pH=3.5 and 6.8 were statistically significant ($P<0.05$). Increase rates of pH 6.8 and 3.5 at the initial time of immersion were followed by constant pH, indicating a reduced dissolution rate.

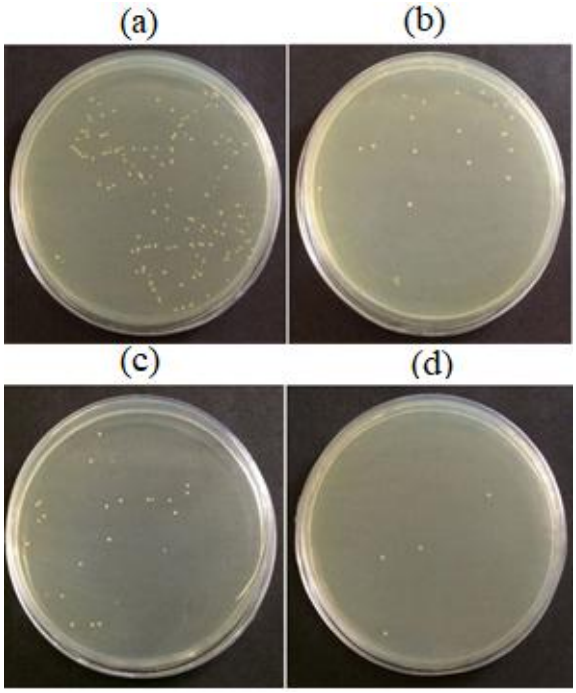

Figure 4. Actual images of the incubated (a, b, c, and d) S.mutans with G1, G2, G3 and G4, respectively.

TABLE 3. The results of S. mutans bacteria colonies

Sample	CFU/ml (start)	CFU/ml (after 24 h)	Antibacterial activity
G1	1.5×10^{8}	1.2×10^{8}	20
G2	1.5×10^{8}	2×10^{6}	83.33
G3	1.5×10^{8}	1.5×10^{6}	87.5
G4	1.5×10^{8}	1×10^{5}	99.17

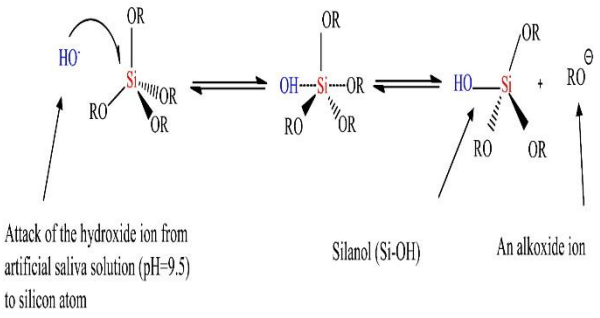

Figure 5. Scheme of dissolution of glass after soaking in basic artificial saliva

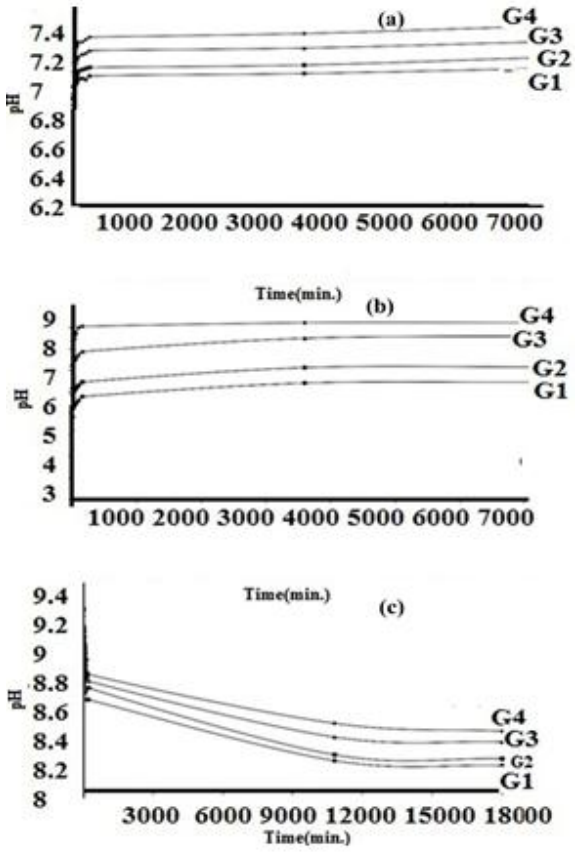

Figure 6. Changes in pH AS solutions after immersion of samples and their insets over initial 2 hours: (a) at pH = 6.8, (b) at pH = 3.5, and (c) at pH = 9.5

Figure 7 shows the formation of silanol groups (Si-OH) on the glass surface caused by ion exchanging.

In Figure 6, the reason for the initial increase in the pH of solutions is the cation exchanges of Ca^{2+}, Na^{+}, and Li^{+} with H^{+} from the solution. Therefore, after the glass immersion in the AS, the pH raises by the following ion exchange reactions and the OH^{-} concentration will be increased [33].

1) $Si\text{-}O\text{-}Na^{+} + H^{+} + OH^{-} \longrightarrow Si\text{-}OH + Na^{+}(aq.) + OH^{-}$
2) $Si\text{-}O\text{-}Li^{+} + H^{+} + OH^{-} \longrightarrow Si\text{-}OH + Li^{+}(aq.) + OH^{-}$
3) $Si\text{-}O\text{-}Ca^{2+} + H^{+} + OH^{-} \longrightarrow Si\text{-}OH + Ca^{2+}(aq.) + OH^{-}$

As the data illustrates, the increase of pH is in order G4>G3>G2>G1, pointing to the fact that fast ion exchanging occurred between Li^{+}-H^{+} in the solution compared to Na^{+}-H^{+} [34].

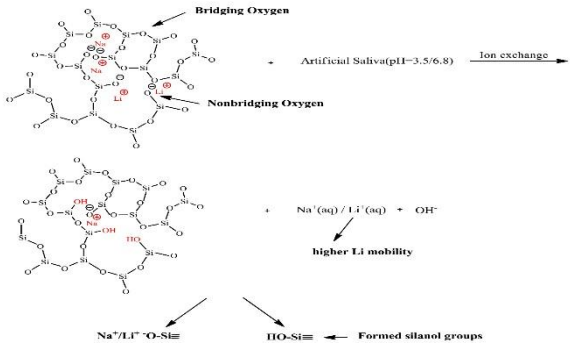

Figure 7. Mechanism of glass degradation after immersion in acidic artificial saliva

Figure 7 shows the pH decrease in AS from 9.5 (in the 3 days) followed by a steady state at long immersion times. The pH variation in AS was significantly different ($P<0.05$). Ca^{2+}, Na^{+}, and Li^{+} disrupt the silicate network by non-bridging oxygen including Si-O- $Li^{+}/Na^{+}/Ca^{2+}$ bonds. Since the association energy of the Li/O bond (340.5 kcal mol) is higher than Na/O (270 kcal mol), Na^{+} ions form more non-bridging oxygen. Thus, durability in basic pH increased by lithium substitution.

In fact, the tendency of basic oxide formation is higher with the decreasing of element electronegativity [23].

Thus, since Li^{+} has higher electronegativity than Na^{+} ion, it will decrease the basicity of the glasses. As a consequence, the reactivity of lithium bearing glass with the acid phases will be reduced.

Figure 8 shows the weight loss of samples in the first week. There was a noticeable difference in degradation for AS ($P<0.05$). In basic media, chemical durability is enhanced by Li in the specimens.

The protection of glasses against degradation in contact with water is a significant clinical success. Consequently, chemical composition, pH storage media, and immersion time have a noticeable effect on degradation of glass.

Figure 9 shows the particle morphology after the soaking in AS solution. After immersion of samples in media solution for 14 days, the surface of particles becomes smoother and their morphologies change to globular, which is associated to glass degradation.

According to the EDS results (Figure 9), the chemical analysis of G4 has not changed (before and after immersion). The reduced degradation rate of glasses was related to the Li water-soluble salts with lower solubility than the sodium water-soluble salts [13, 28]

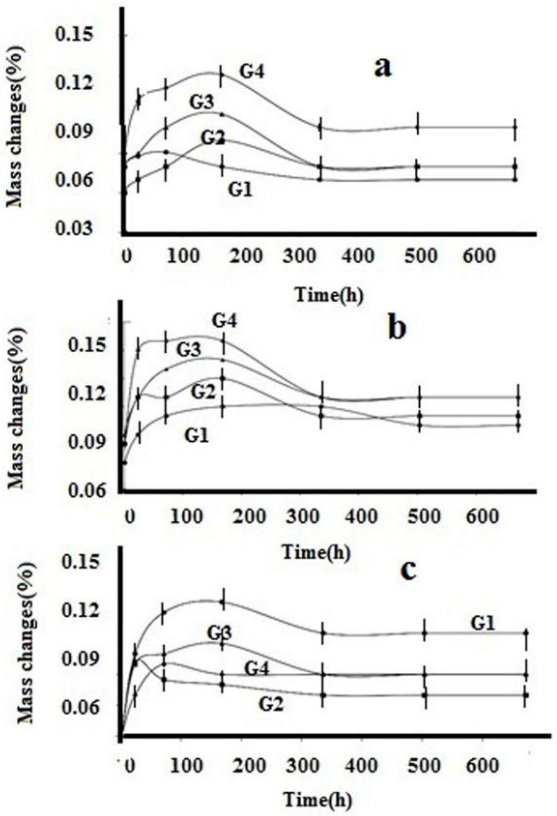

Figure 8. Mass change (Mg%) of glasses immersed in artificial saliva with different pHs over one month: (a) pH = 6.5, (b) pH = 3.5, and (c) pH = 9.5

The frequencies at~ 446 cm^{-1} (attributed to the bending vibration of Si-O-Si , Al-O-Al, and Si-O-Si arised from dissolution of the G4 after soaking in AS for 14 days [2]. The results in Figure 10 point to the break of Si-O-Si and Al-O-Si bonds, bringing about release of network and modifier ions and the solubility of glass [25]. Also, the intensity of the band at ~ 3436.17 decreased after immersion. It is justified that the little exchange between modifier ions and hydrogen ions in media at pH>9 occurs. However, at pH <9, wide ion exchanges should be produced [26].

Figure 11 shows the cytotoxicity of GIC. The results of MTT assay show the cytotoxicity of all GICs against G-292 osteoblasts, in which the effect of GICs on viability of cells was improved by Li substitution. The morphologies of cells cultured for 24 h. in the conditioned medium demonstrated better cell spearing on the modified cement. There is no significant difference between cytotoxicity rates of cements ($P>0.05$).

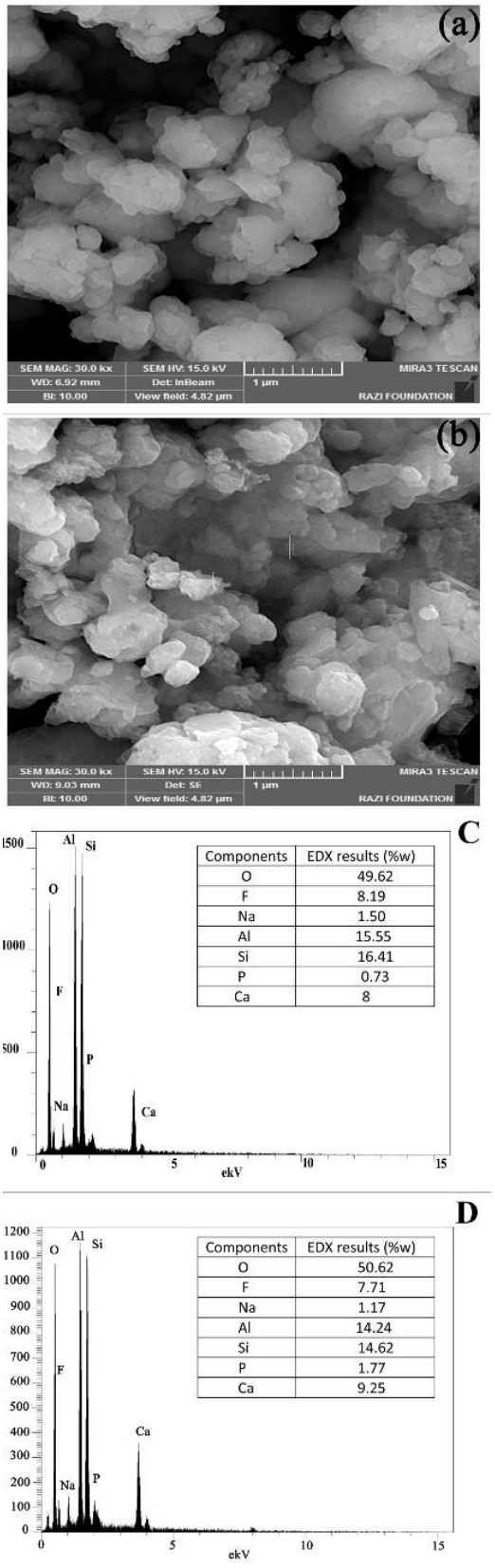

Figure 9. FESEM images and EDS analysis of G4 before (a) and after (b) immersion in artificial saliva for 14 days

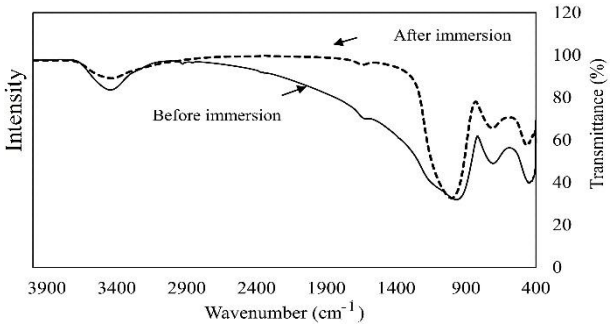

Figure 10. IR spectra of the experimental glass (G4) before and after immersion in AS solution for 14 days

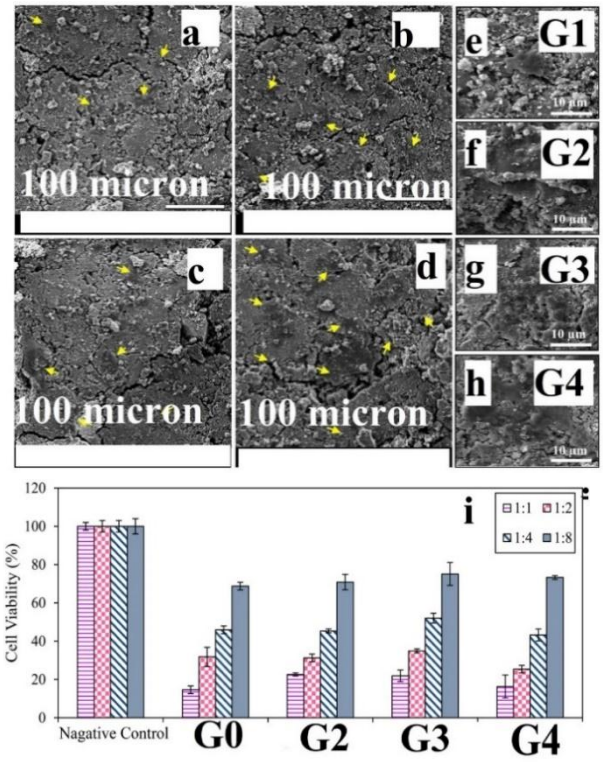

Figure 11. MTT activity of the human osteoblast cells cultured for 24 h in a conditioned medium soaked with cements (G1, G2, G3, and G4) and negative control (diluted by factors 1:2 to 1:8 and undiluted 1:1). SEM images of the human osteoblast (G-292) cells cultured for 24 h in a conditioned medium soaked with cements (a) G1, (b) G2, (c) G3, and (d) G4 with ×1000 magnification, (e) G1, (f) G2, (g) G3, and (h) G4 with 10000 magnification, and (i) the counted Cell in various samples

There was no significant difference in cytotoxicity between experiments ($P>0.05$). The addition of Li to the dilution of 1:1 and MTT activity has higher cell vitality than Li-free cement (Figure 11). However, this difference was not significant by further dilution (1:2, 1:4, and 1:8). As mentioned earlier, GICs were formed by the reaction

between glass powder and aqueous solution. Dissolution of free ion metals such as Al^{3+}, Ca^{2+}, and Na^{+} from the powder to liquid occurred in the mixing process. These ions are non-toxic and do not damage living cells or tissues. Thus, polyacrylic acid in the liquid phase is responsible for cytotoxicity of CICs [34].

4. CONCLUSION

Our research demonstrated the substitution of Li to Na in SiO_2-Al_2O_3-AlF_3-CaF_2-$AlPO_4$-NaF glasses. This study showed that transition temperature, density, network structure, and antibacterial activity were dependent on concentration of Li. G3 (6 wt.% Li) showed higher density than G2 (3 wt.% Li) and G4 (9.2 wt.% Li). The atomic weight or strength field of this ion would be the dominant factor. Also, in Na bearing glass, the disruption of Si-O-Si bonds was hindered by Li. T_g shifted to higher temperatures. It was proved that the breaking of the silicate glasses network in the presence of Na was easier than Li. A decline in the number of non-bridging oxygen was caused by addition of Li. Low atomic weigh of lithium compared to sodium led to the decreased density of synthesized glasses. G4 sample (9.2 wt% Li) showed the highest antibacterial properties. In an acidic environment, the addition of Li to glasses resulted in enhanced solubility. Since breaking Si-O-Si bonds plays a key role in dissolution of glasses in basic pH, the rate of structure disruption was decreased by Li substitution. Justifiably, insigificant exchanges between modifier ions and hydrogen ions in media at pH >9 occurred. However, at pH<9, wide ion exchanges occurred. The observation of FESEM-EDX revealed that the immersion of glass in media solution could make changes in morphologies of the particles caused by the dissolution process.

ACKNOWLEDGEMENT

The author acknowledges the financial support of coating Project, Contract No. 93021874, from Materials and Energy Reasearch Center.

REFERENCES

1. Forss, H., Widström, E., "Reasons for Restorative Therapy and Longevity of Restorations in Adults", ***Acta Odontologica Scandinavica***, Vol. 62, No. 2, (2004), 82-86. https://doi.org/10.1080/00016350310008733
2. Selwitz, R. H., Ismail, A. I., Pitts, N. B., "Dental Caries", ***The Lancet***, Vol. 369, No. 9555, (2007), 51-59. https://doi.org/10.1016/S0140-6736(07)60031-2
3. Hengtrakool, C., Pearson, G. J., Wilson, M., "Interaction Between GIC and S. Sanguis Biofilms: Antibacterial Properties and Changes of Surface Hardness", ***Journal of Dentistry***, Vol. 34, No. 8, (2006), 588-597. https://doi.org/10.1016/j.jdent.2005.02.011
4. Kidd, E. A. M., Fejerskov, O., "What Constitutes Dental Caries? Histopathology of Carious Enamel and Dentin Related to the Action of Cariogenic Biofilms", ***Journal of Dentistry Research***, Vol. 83, No. 1_suppl, (2004), 35-38. https://doi.org/10.1177/154405910408301s07
5. Van Houte, J., Lopman, J., Kent, R., "The Predominant Cultivable Flora of Sound and Carious Human Root Surfaces", ***Journal of Dental Research***, Vol .73, No. 11, (1994), 1727-1734. https://doi.org/10.1177/00220345940730110801
6. Caufield, P. W., Li, Y., Dasanayake, A., "Dental caries: an infectious and transmissible disease", ***Compendium of Continuing Education in Dentistry (Jamesburg, NJ: 1995)***, Vol. 26, No. 5 Suppl 1, (2005), 10-16. PMID: 17036539. https://pubmed.ncbi.nlm.nih.gov/17036539/
7. Yip, K., Smales, R., "Oral diagnosis and treatment planning: part 2. Dental caries and assessment of risk", ***British Dental Journal***, Vol. 213, No. 2, (2012), 59-66. https://doi.org/10.1038/sj.bdj.2012.615.
8. Zamanian, A., Yasaei, M., Ghaffari, M., Mozafari, M., "Calcium hydroxide-modified zinc polycarboxylate dental cements", ***Ceramics International***, Vol. 39, No. 8, (2013), 9525–9532. https://doi.org/10.1016/j.ceramint.2013.05.071
9. Yasaei, M., Zamanian, A., Moztarzadeh, F., Ghaffari, M., Mozafari, M., "Characteristics improvement of calcium hydroxide dental cement by hydroxyapatite nanoparticles. Part 1: formulation and microstructure", ***Biotechnology and Applied Biochemistry***, Vol. 60, No. 5, (2013), 502-509. https://doi.org/10.1002/bab.1119PMID: 23586755
10. Farrugia, C., Camilleri, J., "Antimicrobial properties of conventional restorative filling materials and advances in antimicrobial properties of composite resins and glass ionomer cements-A literature review", ***Dental Materials***; Vol. 31, No. 4. (2015), e89-e99. https://doi.org/10.1016/j.dental.2014.12.005
11. Zamanian, A., Moztarzadeh, F., Kordestani, S., Hesaraki, S., Tahriri, M. R., "Novel calcium hydroxide/nanohydroxyapatite composites for dental applications: In vitro study", ***Advances in Applied Ceramics***, Vol. 109, No. 7, (2010), 440-444. https://doi.org/10.1179/174367610X12804792635107
12. Wilson, A. D., Kent, B. E., "The glass-ionomer cement, a new translucent cement dental filling material", ***Journal of Applied Chemistry and Biotechnology,*** Vol. 21, No. 11, (1971), 313. https://doi.org/10.1002/jctb.5020211101
13. Moshaverinia, A., Roohpour, N., Chee, W. W., Schricker, S. R., "A review of powder modifications in conventional glass-ionomer dental cements", ***Journal of Materials Chemistry***, Vol. 21, No. 5, (2011), 1319-1328. https://doi.org/10.1039/C0JM02309D
14. Agha, A., Parker, S., Patel, M. P., "Development of Experimental Resin Modified Glass Ionomer Cements (RMGICs) with Reduced Water uptake and Dimensional Change", ***Dental Materials***, Vol. 32, No. 6, (2016), 713-722. https://doi.org/10.1016/j.dental.2016.03.004.
15. Weidlich, P., Miranda, L. A., Maltz, M., Samuel, S. M., "Fluoride release and uptake from glass ionomer cements and composite resins", ***Brazilian Dental Journal***, Vol. 11, No. 2, (2000), 89-96. http://www.forp.usp.br/bdj/bdj11(2)/t03112/t03112.html
16. Vermeersch, G., Leloup, G., Vreven, J., "Fluoride release from glass-ionomer cements, compomers and resin composites", ***Journal of Oral Rehabilitation***, Vol. 28, No. 1, (2001), 26-32. https://doi.org/10.1046/j.1365-2842.2001.00635.x.
17. Manhart, J., García-Godoy, F., Hickel, R., "Direct posterior restorations: Clinical results and new developments", ***Dental Clinics of North America***, Vol. 46, No. 2, (2002), 303-339. https://doi.org/10.1016/S0011-8532(01)00010-6.
18. Randall, R. C., Wilson, N. H. F., "Glass-ionomer restoratives: A systematic review of a secondary caries treatment effect", ***Journal of Dental Research***, Vol. 78, No. 2, (1999), 628-637. https://doi.org/10.1177/00220345990780020101.

19. Hu , J., Du, X., Huang, C., Fu, D., Ouyang, X., Wang, Y., "Antibacterial and physical properties of EGCG-containing glass ionomer cements", ***Journal of Dentistry***, Vol. 41, No. 10, (2013), 927-934. https://doi.org/:10.1016/j.jdent.2013.07.014.
20. Xie, D., Weng, Y., Guo, X., Zhao, J., Gregory, R. L., Zheng, C., "Preparation and evaluation of a novel glass-ionomer cement with antibacterial functions", ***Dental Materials***, Vol. 27, No .5, (2011), 487-496. https://doi.org/ 10.1016/j.dental.2011.02.006.
21. Somani, R., Jaidka, S., Jawa, D., Mishra, S., "Comparative evaluation of microleakage in conventional glass ionomer cements and triclosan incorporated glass ionomer cements", ***Contemporary Clinical Dentistry***, Vol. 5, No. 1, (2014), 85-88. https://doi.org/10.4103/0976-237X.128675.
22. Shaiksha Vali, K., Murugan, B. S., Reddy, S. K., Noroozinejad Farsangi, E., "Eco-friendly Hybrid Concrete Using Pozzolanic Binder and Glass Fibers", ***International Journal of Engineering***, Vol. 33, No. 7, (2020), 1183-1191. https://dx.doi.org/10.5829/ije.2020.33.07a.03.
23. Rasti; M., Hesaraki; S., Nezafati, N., "An investigation on injectable composites fabricated by 45S5 bioactive glass and gum tragacanth: Rheological properties and in vitro behavior", ***Advanced Ceramic Progress***, Vol. 4, No. 2, (2018), 16-26. https://doi.org/10.30501/acp.2018.91121
24. Mosbahi, S., Oudadesse, H., Wers, E., Trigui, M., Lefeuvre, B., Roiland, C., Elfeki, H., Elfeki, A., Rebai, T., Keskes, H., "Study of bioactive glass ceramic for use as bone biomaterial in vivo: Investigation by nuclear magnetic resonance and histology", ***Ceramics International***, Vol. 42, No. 4, (2016), 4827-4836. https://doi.org/10.1016/j.ceramint.2015.11.168
25. Huang, X., Yang, T., Zhao, S., Huang, C., Du, X., "Anti-biofilm effect of glass ionomer cements incorporated with chlorhexidine and bioactive glass", ***Journal of Wuhan University of Technology-Materials Science Edition***, Vol. 27, No. 2, (2012), 270–275. https://doi.org/10.1007/s11595-012-0451-1
26. Elsaka, S. E., Hamouda, I. M., Swain, M. V., "Titanium dioxide nanoparticles addition to a conventional glass-ionomer restorative: influence on physical and antibacterial properties", ***Journal of Dentistry***, Vol. 39, No. 9, (2011), 589-598. https://doi.org/10.1016/j.jdent.2011.05.006
27. Lieb, J., "Lithium and antidepressants: stimulating immune function and preventing and reversing infection", ***Medical Hypotheses***, Vol. 69, No. 1, (2007), 10-11. https://doi.org/10.1016/j.mehy.2006.12.005
28. Kavitha, R. J., Subha, B., Shanmugam, S., Ravichandran, K., "Synthesis and Invitro Characterisation of Lithium Doped Bioactive Glass through Quick Alkali Sol-Gel Method", (***IJIRSE) International Journal of Innovative Research in Science & Engineering***, Vol. 2, (2014), 2347-3207. https://www.researchgate.net/publication/265249136_Synthesis_and_Invitro_Characterisation_of_Lithium_Doped_Bioactive_Glass_through_Quick_Alkali_Sol-Gel_Method
29. Wang, J., de Boer, J., de Groot, K., "Proliferation and differentiation of osteoblast-like MC3T3-E1 cells on biomimetically and electrolytically deposited calcium phosphate coatings", ***Journal of Biomedical Materials Research Part A: An Official Journal of The Society for Biomaterials, The Japanese Society for Biomaterials, and The Australian Society for Biomaterials and the Korean Society for Biomaterials***, Vol. 90, No. 3, (2009), 664-670. https://doi.org/10.1002/jbm.a.32128
30. Hesaraki, S., Gholami, M., Vazehrad, S., Shahrabi, S., "The effect of Sr concentration on bioactivity and biocompatibility of sol–gel derived glasses based on $CaO–SrO–SiO_2–P_2O_5$ quaternary system", ***Materials Science and Engineering: C***, Vol. 30, No. 3, (2010), 383-390. https://doi.org/10.1016/j.msec.2009.12.001
31. Akashi, A., Matsuya, Y., Unemori, M ., Akamine, A., "The relationship between water absorption characteristics and the mechanical strength of resin-modified glass-ionomer cements in long-term water storage", ***Biomaterials***, Vol. 20, No. 17 , (1999), 1573-1578. https://doi.org/10.1016/S0142-9612(99)00057-5
32. Hanting, C., Hanxing, L., Guoqing, Z., "The setting chemistry of glass ionomer cemen", ***Journal of Wuhan University of Technology- Materials Science Edition***, Vol. 20, No. 4, (2005), 110–112. https://doi.org/10.1007/BF02841298
33. Kaur, M., Singh, S. P., Mudahar, D. S., Mudahar, G. S., "Structural B_2O_3-Li_2CO_3-Al_2O_3 Glasses By Molar Volume Measurements and FTIR Spectroscopy", ***Materials Physics and Mechanics***, Vol. 15, (2012), 66-73. http://mp.ipme.ru/e-journals/MPM/no_11512/MPM115_06_kaur.pdf
34. Sayyedan, F. S., Fathi, M., Edris, H., Doostmohammadi, A., Mortazavi, V., Shirani, F., "Fluoride release and bioactivity evaluation of glass ionomer: Forsterite nanocomposite", ***Dental Research Journal***, Vol. 10, No. 4, (2013), 452-459. https://www.ncbi.nlm.nih.gov/pmc/articles/PMC3793407/